ESAIM: PROCEEDINGS AND SURVEYS, Vol. ?, 2019, 1-10
Editors: Will be set by the publisher

MODELING THE SPATIAL PROPAGATION OF Aβ OLIGOMERS IN ALZHEIMER'S DISEASE

Martin Andrade-Restrepo[1], Paul Lemarre[2, 3], Laurent Pujo-Menjouet[2,3], Leon Matar Tine[2,3] and Sorin Ionel Ciuperca[2]

Abstract. Recent advances in the study of Alzheimer's Disease and the role of Aβ amyloid formation have caused the focus of biologists to progressively shift towards the smaller protein assemblies, the oligomers. These appear very early on in the disease progression and they seem to be the most infectious species for the neurons. We suggest a model of spatial propagation of Aβ oligomers in the vicinity of a few neurons, without considering the formation of large fibrils or plaques. We also include a simple representation of the oligomers neurotoxic effect. A numerical study reveals that the oligomers spatial dynamics are very sensitive to the balance between their diffusion and their replication, and that the outcome in terms of the progression of AD strongly depends on it.

Résumé. Au cours des dernières années, la recherche sur la maladie d'Alzheimer a révélé l'importance des oligomères d'Aβ dans le développement de la pathologie. Ces structures de petite taille, en comparaison aux fibrilles et aux plaques amyloïdes, apparaissent au cours des toutes premières étapes de la maladie et semblent être les espèces les plus toxiques pour les neurones. En conséquence, nous proposons un modèle de propagation spatiale des oligomères dans le voisinage de quelques neurones, sans considérer la présence de plus grandes structures. La toxicité des oligomères est aussi modélisée de façon simplifiée. L'étude numérique de ce modèle nous permet de mettre en évidence l'influence critique de l'équilibre entre diffusion et réplication des oligomères sur leur répartition spatiale, et la progression de la maladie d'Alzheimer en dpend fortement.

Introduction

Biological background: Alzheimer's Disease and Aβ aggregation

Alzheimer's disease (AD) is the most common of neurodegenerative diseases, a group also including Parkinson's disease, Huntington disease, Creutzfeldt-Jakob disease, transmissible spongiform encephalopathies. As is the case for these other diseases, AD is associated with the misconformation, aggregation and propagation of different proteins in the neural system [24], namely the proteins Aβ and tau. The distinct characteristic of these proteins is their ability to adopt different stable **conformations**. Misshapen conformations often lead to **aggregation** and accumulation of the proteins into assemblies of different structure, stability and activity.

Biologists identify two different types of structures. On one hand the proteins can assemble into long linear **fibrils**. These fibrils in turn coalesce into large and amorphous tangles, that constitute the visible **plaques**

[1] Institut Jacques Monod, CNRS UMR 7592, Université Paris Diderot, Paris Cité Sorbonne, F-750205, Paris, France.
[2] Institut Camille Jordan, Université de Lyon, Université Claude Bernard Lyon 1, CNRS UMR 5208, 43 blvd. du 11 novembre 1918, 69622 Villeurbanne cedex, France
[3] Team Dracula, INRIA, 69603 Villeurbanne Cedex, France

observed in most late-stage AD patients. On the other hand, they can also assemble into smaller oligomeric species. These **oligomers** are soluble, and thus more difficult to detect, but their role in AD propagation and pathology is believed to be essential [13, 23]. In fact, in the last decade it has become clear that plaques are mostly inactive by-products of polymerization, but oligomers are the active species both for propagation inside the brain and destruction of the neurons. The interaction between fibrils and oligomers is unclear, but it has been shown that oligomers appear early on during the onset of Alzheimer's disease, while fibrils and plaques become detectable much later [13].

The generally accepted mechanism for the onset of AD is the so-called **cascade hypothesis** [7, 13]. The first appearance of oligomers is a rare and highly stochastic event, possibly favored by mutations or co-factors. Monomers can spontaneously change conformation and assemble into small proto-oligomers, this process is termed primary nucleation. Once the process has started and a seed has appeared, the oligomers replicate very fast [7, 19, 22, 25]. This second step is usually referred to as secondary nucleation. Although the precise phenomenon that allows oligomers to replicate is not known, it can be described as a prion-like propagation. A combination of propagation in the brain through diffusion, recruitment of healthy Aβ monomers, and though other mechanisms such as exosomes [27]. In the later stages, fibrils and plaques accumulate in the brain.

It is of particular interest for biologists and physicians to understand the precise mechanisms of propagation and replication of Aβ oligomers, especially in the early stages of AD. Insight into the phenomena could indeed help develop therapeutical strategies [9, 13], favor early diagnosis and predict the prognosis of the pathology. This is precisely where our focus lies, at the very early stages of the disease when a seed has been produced and oligomers start replicating.

Previous mathematical work

Amyloid formation and propagation has drawn strong attention among scientists and has been the subject of numerous interdisciplinary research studies. In particular, numerical and mathematical modeling, both stochastic and deterministic has aimed to shed light on the subject. Early modeling work used systems of ordinary or partial differential equations to study the dynamics of prion aggregates [8, 12, 17] in the context of transmissible spongiform encephalopathies (TSE). The dynamics of Aβ oligomers and prion aggregates are similar, however different microscopic processes distinguish the two.

A more recent discovery is that Aβ oligomers interact with the prion protein (PrP) to induce neurotoxicity, and different models of joint PrP-Aβ dynamics have been introduced [6, 15, 16]. These models propose an elaborate description of the degenerative effect oligomers have on the neurons, but they do not analyze the effects of their spatial spreading. In [6,15], a size-continuous description of the aggregates is used, and while the latter can be a good approximation for very large aggregates it is less relevant for small oligomers. The relation between continuous and discrete protein sizes has been studied rigorously in [8, 26, 28]. In [16], the size of the oligomers, fibrils and plaques is discrete. Overall, the molecular dynamics of oligomers have been investigated in the context of general models where fibrils and plaques were also present, and with a complex description of neurotoxicity involving the prion protein.

The spatial dynamics of aggregated species have been analyzed for Alzheimer's Disease [3], and for prion propagation in other neurodegenerative disorders [5]. In [3] a comprehensive model of amyloid spatial propagation in the form of Aβ monomers, oligomers, fibrils (and plaques) was introduced. While this model achieves some interesting results in the qualitative dynamics of macroscopic biomarkers (deposits and brain atrophy), some of the parameters and hypotheses remain unjustified biologically. In particular, the extrapolation of microscopic molecular dynamics to a macroscopic scale is delicate, because different biological processes have to be taken into account at the macroscopic scale (*e.g.* the recycling of cerebrospinal fluid).

In this work we intend to develop a model similar to the one proposed in [16], with a special focus on Aβ oligomers and their spatial propagation. The scope of this model is the early stages of AD propagation, when fibrils and plaques are most likely not yet present and the dynamics are driven by oligomers. As studied in [3] we include diffusion of the different molecular species, but we restrict the study to the mesoscopic scale (a few neurons), which is also relevant with the early stages of the disease. This ensures that our hypothesis of

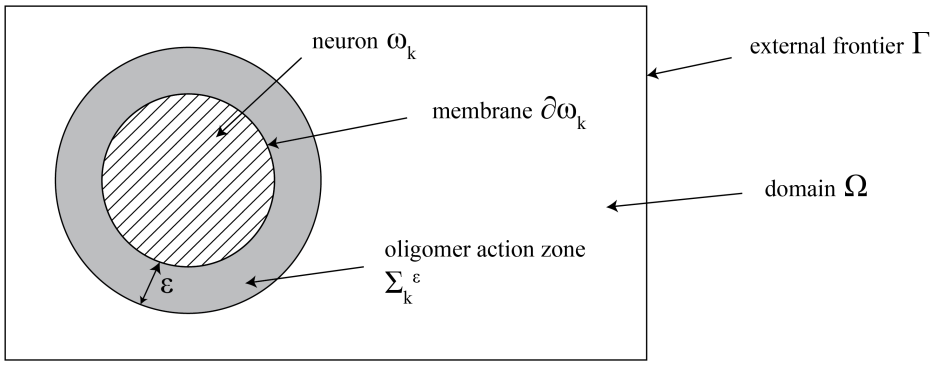

FIGURE 1. Representation of the modeling domain (with only one neuron represented)

absence of fibrils or plaques is valid. To simplify even further the model, the neurotoxicity of the oligomers is considered independently of any other protein. These hypotheses allow us to build a simpler model, at the cost of restricting the scope, but with a stronger biological basis.

In the first section, we introduce the biological model as well as its mathematical formulation. This formulation is presented as a partial differential equation problem and its variational formulation. The second section describes some preliminary theoretical results. The third section discusses the parameter choice, before showing simulation results.

1. A SPATIAL MODEL OF Aβ OLIGOMERS

1.1. Model hypotheses and formulation

We investigate a simplified model of the propagation of Aβ oligomers in the brain. We do not aim at modeling the spontaneous appearance of oligomers in the brain. This sporadic event is highly stochastic and rare, but once it is seeded, the proliferation of oligomers becomes very fast and deterministic. We aim here at describing the evolution of a small initial number of oligomers in the vicinity of a few neurons (mesoscopic scale) using partial differential equations. Fibrils and plaques are not considered yet, since they are not believed to appear until a later stage of the disease.

1.1.1. *Molecular scale*

First we describe the chemical processes that we consider at the molecular scale. We consider a domain Ω with a boundary Γ, where $N \in \mathbb{N}$ **neurons** $\omega_1, \omega_2, ..., \omega_N$ are represented by disks. Fig. 1 shows a representation of one neuron in the domain Ω. The neurons actively produce **Aβ monomers** with a rate λ at their membrane $\partial\omega_k$, $k = 1, 2, ..., N$. The Aβ monomer production rate is homogeneous along the membrane of one neuron but depends on its activity. The significance and the evolution of this activity will be described later on. The Aβ monomers inside Ω are constantly evacuated or degraded by the cerebro-spinal fluid with a rate δ.

The Aβ monomers assemble first into **proto-oligomers**, and then **oligomers**. Proto-oligomers are small unstable polymers that grow by addition of monomers - **polymerization** - with a rate r_i (for size i), and that lose monomers through **depolymerization** with a rate b. The polymerization rate is supposed to be size dependent, whereas the depolymerization rate is not. Proto-oligomers can also **fragment** into smaller pieces. We assume that each bond in a proto-oligomer is equally likely to break. This implies that the fragmentation

rate grows linearly with size, a proto-oligomer of size i will fragment at rate $\beta \times (i-1)$. It also implies that the fragmentation kernel $\kappa(i,j)$ (probability of obtaining a size i aggregate from a size j aggregate) is uniform. This writes as $\kappa(i,j) = \frac{1}{j-1}\mathbb{1}_{[1\leq i\leq j-1]}$ [8] (it does not depend on i). Note that such a fragmentation kernel verifies the following usual properties

- Symmetry: $\kappa(i,j) = \kappa(j-i,j)$
- Probability kernel: $\sum_{i=1}^{j-1}\kappa(i,j) = 1$ (which implies $\kappa(i,j) = 0$ for $i \geq j$)
- Mass conservation: $2\sum_{i=1}^{j-1} i\kappa(i,j) = j$ (the factor 2 comes from the symmetry property)

Using this kernel greatly simplifies the fragmentation equation. Indeed, expressing the speed of fragmentation from size j to size i gives $2\beta(j)\kappa(i,j) = 2\beta$ for $1 \leq i \leq j-1$ (the factor 2 once again comes from the symmetry of the kernel). This model is the classical polymerization-fragmentation equation, see [12, 17] for further developments.

Once proto-oligomers reach the critical size i_0, they become oligomers. The oligomers are very stable units that do not exchange monomers with the system, as suggested in previous models [16]. This means that they neither depolymerize nor fragment. We assume that they are the main toxic elements for the neurons.

The above assumptions are illustrated in Figure 2. They are also summarized into the following set of chemical reactions, where m is the local density of monomers, μ_i is the local density of size i proto-oligomers ($\mu_1 = m$ by convention), and μ_{i_0} that of oligomers.

$$\begin{aligned}
&\forall k \in \{1,\dots,N\}, \forall x \in \partial\omega_k, && \emptyset \xrightarrow{\lambda_k} \mathrm{m},\\
&\forall x \in \Omega, && \mathrm{m} \xrightarrow{\delta} \emptyset,\\
&\forall x \in \Omega, \forall i \in \{2,\dots,i_0-2\}, && \mu_i + \mathrm{m} \underset{\mathrm{b}}{\overset{\mathrm{r_i}}{\rightleftharpoons}} \mu_{i+1},\\
&\forall x \in \Omega, && \mu_{i_0-1} + \mathrm{m} \xrightarrow{\mathrm{r_{i_0-1}}} \mu_{i_0},\\
&\forall x \in \Omega, \forall j \in \{2,\dots,i_0-1\}, \forall i \in \{1,\dots,j-1\}, && \mu_j \xrightarrow{\beta\times(\mathrm{j\text{-}1})} \mu_i + \mu_{j-i}.
\end{aligned}$$

1.1.2. *Mesoscopic scale*

We now describe the interactions between the different molecular elements at the mesoscopic scale. Naturally, we are interested in studying more than one neuron. The objective here is to describe how the polymerization reaction propagates from neuron to neuron via diffusion and induces progressive neurodegeneration.

On the scale of a few neurons, we consider spatial diffusion of all the molecular components described before, in two dimensions. The choice of two dimensions instead of three is a simplification that allows for easier numerical simulations. The main consequence is that the spacing of neurons needs to be adjusted, as well as the diffusion coefficient in order to model the behavior of proteins in an actual three-dimensional environment. However, if we assume that diffusion in the brain is isotropic, the qualitative properties of the two-dimensional model are similar to the three-dimensional model. Each species is associated with a specific diffusion coefficient depending on its size, from D_1 (for $A\beta$ monomers) to D_{i_0} for oligomers. We assume that the smaller the species, the faster it is diffused. The specific choice of the diffusion coefficients and their scaling with size will be described later on.

Oligomers are supposed to be the toxic species. Their effect on the neurons relies on their presence in the action perimeter Σ_k^ε of radius ε around ω_k (see Figure 1). To model the fact that oligomers progressively kill the neurons, we use an equation to describe their production rate. A healthy neuron produces $A\beta$ monomers at maximum rate λ_0, and a dead neuron has a production rate of 0. We suggest that this production decreases

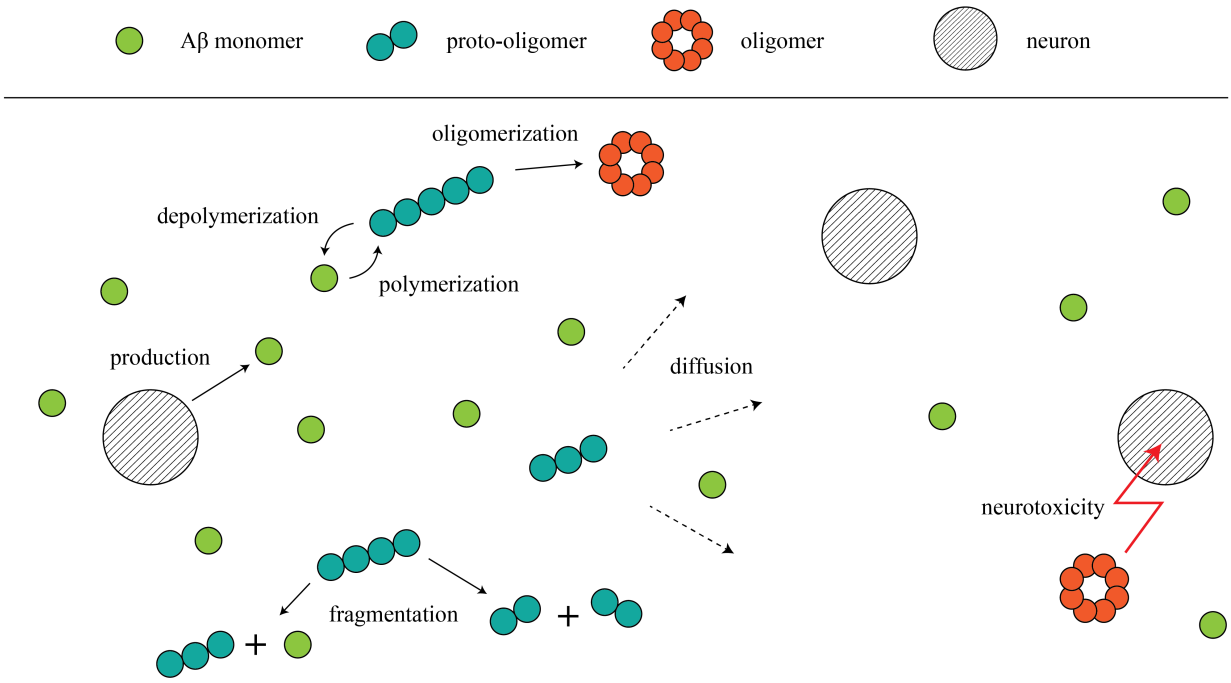

FIGURE 2. Representation of the different processes and agents at play in the model

with a rate proportional to the number of oligomers in the ring Σ_k^ε. A simple model to describe this is

$$\frac{\mathrm{d}\lambda_k}{\mathrm{d}t} = -\tau\lambda_k \int_{\Sigma_k^\varepsilon} \mu_{i_0}(x,t)\,\mathrm{d}x.$$

Here τ represents the lethal efficiency of the oligomers on the neurons. Our model implies that neurons can only degenerate, with no chance of recovery from the toxicity inflicted by oligomers. This hypothesis will be questioned in detail in future developments. This choice of behavior for the neurons implies that the outcome of any simulation that starts with a positive amount will converge towards a situation where all neurons in presence are inactive.

As said previously, the production of Aβ happens only at the surface membrane of the neurons $\partial\omega_k$. This gives the boundary condition for monomers on these surfaces, via a non-homogeneous Neumann condition. For the other species (proto-oligomers and oligomers), we consider a simple non-flux boundary condition.

On the sides of the domain Ω, different choices are possible. To model isolation from other neurons, we can use absorbing conditions on the external boundary, but we could also consider periodical boundary conditions to reflect the effect of a crowded brain region. For the moment, we choose an absorbing condition.

1.2. **Mathematical formulation**

1.2.1. *System of partial differential equations*

We now introduce the mathematical problem corresponding to the model, first the local equations, then the boundary conditions and finally the initial condition. Our goal here is to discuss the hypotheses made in the

formulation of the model, and not provide general theoretical results. For this reason we do not specify the formal and general mathematical problem in this work. It will be done as part of a subsequent theoretical study.

The local densities of the different elements verify the following system of partial differential equations for $x \in \Omega$ and $t > 0$

$$\begin{aligned}
\frac{\partial m}{\partial t}(x,t) =& D_1 \Delta m + \sum_{j=3}^{i_0-1} b\mu_j - \sum_{j=2}^{i_0-1} r_j \mu_j m + 2\beta \sum_{j=2}^{i_0-1} \mu_j - \delta m, \\
\frac{\partial \mu_2}{\partial t}(x,t) =& D_2 \Delta \mu_2 + b\mu_3 - r_2 \mu_2 m - \beta \mu_2 + 2\beta \sum_{j=3}^{i_0-1} \mu_j, \\
\forall i \in \{3, \dots, i_0 - 2\}, \frac{\partial \mu_i}{\partial t}(x,t) =& D_i \Delta \mu_i + b\mu_{i+1} - b\mu_i + r_{i-1}\mu_{i-1} m - r_i \mu_i m - \beta(i-1)\mu_i + 2\beta \sum_{j=i+1}^{i_0-1} \mu_j, \\
\frac{\partial \mu_{i_0-1}}{\partial t}(x,t) =& D_{i_0-1} \Delta \mu_{i_0-1} - b\mu_{i_0-1} + r_{i_0-2}\mu_{i_0-2} m - r_{i_0-1}\mu_{i_0-1} m - \beta(i_0-2)\mu_{i_0-1}, \\
\frac{\partial \mu_{i_0}}{\partial t}(x,t) =& D_{i_0} \Delta \mu_{i_0} + r_{i_0-1}\mu_{i_0-1} m.
\end{aligned} \tag{1}$$

The initial conditions are chosen in the space $X = \{v \in \mathrm{L}^2(\Omega) | v(x) \geq 0, \ a.e.\ x \in \Omega, \}$.

$$\begin{aligned}
&a.e. x \in \Omega, m(x,0) = m^0(x), \mu_2(x,0) = \mu_2^0(x), \dots, \mu_{i_0}(x,0) = \mu_{i_0}^0(x), \\
&\{m^0, \mu_2^0, \dots, \mu_{i_0}^0\} \in X^{i_0}.
\end{aligned} \tag{2}$$

All the boundary conditions we define are Neumann conditions, imposed upon the fluxes of particles. The unitary normal vectors used for these definitions are pointing outwards (relative to the domain Ω), denoted $\vec{n}|_\Gamma$ on the exterior boundary Γ and $\vec{n}|_{\partial\omega_k}$ on the neurons membrane.

On the exterior frontier, we impose an absorbing condition with a proportion γ. This gives, for any variable $\xi = m, \mu_2, \dots, \mu_{i_0}$

$$D_\xi \nabla \xi \cdot \vec{n}|_\Gamma = -\gamma \xi. \tag{3}$$

On the neurons membrane $\partial\omega_k$ for $k \in \{1, \dots, N\}$, we have a zero-flux condition for $\xi = \mu_2, \dots, \mu_{i_0}$ and a source term for m

$$D_\xi \nabla \xi \cdot \vec{n}|_{\partial\omega_k} = 0, \tag{4}$$

$$D_1 \nabla m \cdot \vec{n}|_{\partial\omega_k} = \lambda_k(t). \tag{5}$$

The source term λ_k of the neuron k follows the differential equation

$$\begin{aligned}
\frac{\mathrm{d}\lambda_k}{\mathrm{d}t}(t) =& -\tau \lambda_k \int_{\Sigma_k^\varepsilon} \mu_{i_0}(x,t)\, \mathrm{d}x, \\
\lambda_k(0) =& \lambda_0.
\end{aligned} \tag{6}$$

The initial condition for System (1) is a perturbation of the disease-free solution. The disease-free solution corresponds to the case when no proto-oligomers or oligomers are present, and the neurons are healthy. The monomer density thus verifies the boundary-condition problem

$$\begin{aligned}
D_1 \Delta m =& \delta m, \\
D_1 \nabla m \cdot \vec{n}|_\Gamma =& -\gamma m, \\
\forall k \in \{1, \dots, N\}, D_1 \nabla m \cdot \vec{n}|_{\partial\omega_k} =& \lambda_0.
\end{aligned} \tag{7}$$

The initial condition for m is chosen to be the solution to System (7). The initial condition for proto-oligomers and oligomers is a local Gaussian distribution, both in space and in size of assemblies. This represents the fact that the stochastic process of spontaneous misfolding and oligomerization has already occurred, and a seed is now present to catalyze the reaction.

1.2.2. *Variational formulation*

To run numerical simulations of this system of equations, we use the finite elements method. The first step is to express the problem under a variational form. The calculations that follow are formal, and we assume sufficient regularity for all the functions studied. The theoretical setting will be detailed in future work.

We rewrite System (1) as a system of reaction-diffusion equations (where by convention $\mu_1 = m$)

$$\begin{cases} \forall i \in \{1, \dots, i_0\}, \dfrac{\partial \mu_i}{\partial t} = D_i \Delta \mu_i + F_i(\mu_1, \dots, \mu_{i_0}), \\ \forall i \in \{1, \dots, i_0\}, D_i \nabla \mu_i \cdot \vec{n}|_\Gamma = -\gamma \mu_i, \\ \forall i \in \{2, \dots, i_0\}, D_i \nabla \mu_i \cdot \vec{n}|_{\partial \omega_k} = 0, \text{ and } D_1 \nabla \mu_1 \cdot \vec{n}|_{\partial \omega_k} = \lambda_k(t). \end{cases}$$

The reaction terms are explicitly given by

$$\begin{cases} F_1(\mu_1, \dots, \mu_{i_0}) = -\delta \mu_1 + b \displaystyle\sum_{j=3}^{i_0-1} \mu_j + 2\beta \sum_{j=2}^{i_0-1} \mu_j - \sum_{j=2}^{i_0-1} r_j \mu_j \mu_1, \\ F_2(\mu_1, \dots, \mu_{i_0}) = b\mu_3 - r_2 \mu_2 \mu_1 - \beta \mu_2 + 2\beta \displaystyle\sum_{j=3}^{i_0-1} \mu_j, \\ F_i(\mu_1, \dots, \mu_{i_0}) = b\mu_{i+1} - b\mu_i + r_{i-1}\mu_{i-1}\mu_1 - r_i \mu_i \mu_1 - \beta(i-1)\mu_i + 2\beta \displaystyle\sum_{j=i+1}^{i_0-1} \mu_j, \\ F_{i_0-1}(\mu_1, \dots, \mu_{i_0}) = -b\mu_{i_0-1} + r_{i_0-2}\mu_{i_0-2}\mu_1 - r_{i_0-1}\mu_{i_0-1}\mu_1 - \beta(i_0-2)\mu_{i_0-1}, \\ F_{i_0}(\mu_1, \dots, \mu_{i_0}) = r_{i_0-1}\mu_{i_0-1}\mu_1. \end{cases}$$

To discretize this system in time, we use an Euler scheme with implicit diffusion and explicit reaction. For a pace δ_t and at step n, it writes

$$\frac{\mu_i^{n+1} - \mu_i^n}{\delta_t} = D_i \Delta \mu_i^{n+1} + F_i(\mu_1^n, \dots, \mu_{i_0}^n).$$

By multiplying with a suitable test function, and integrating over the whole domain we get

$$\int_\Omega (\mu_i^{n+1} v - \mu_i^n v)\,\mathrm{d}x - \int_\Omega \delta_t D_i \Delta \mu_i^{n+1} v\,\mathrm{d}x - \int_\Omega \delta_t F_i(\mu_1^n, \dots, \mu_{i_0}^n) v\,\mathrm{d}x = 0.$$

By the divergence theorem we are left with

$$\begin{aligned} \int_\Omega (\mu_i^{n+1} v + \delta_t D_i \nabla \mu_i^{n+1} \cdot \nabla v)\,\mathrm{d}x - \int_\Gamma \delta_t D_i (\nabla \mu_i^{n+1} \cdot \vec{n}) v\,\mathrm{d}x - \sum_k \int_{\partial \omega_k} \delta_t D_i (\nabla \mu_i^{n+1} \cdot \vec{n}) v\,\mathrm{d}x \\ - \int_\Omega \mu_i^n v\,\mathrm{d}x - \int_\Omega \delta_t F_i(\mu_1^n, \dots, \mu_{i_0}^n) v\,\mathrm{d}x = 0. \end{aligned}$$

The boundary conditions give us the variational formulation for each variable $i = 2, \dots, i_0$

$$\int_\Omega (\mu_i^{n+1} v + \delta_t D_i \nabla \mu_i^{n+1} \cdot \nabla v)\,\mathrm{d}x + \int_\Gamma \delta_t \gamma \mu_i^{n+1} v\,\mathrm{d}x - \int_\Omega \mu_i^n v\,\mathrm{d}x - \int_\Omega \delta_t F_i(\mu_1^n, \dots, \mu_{i_0}^n) v\,\mathrm{d}x = 0, \tag{8}$$

and for the monomers

$$\begin{aligned}\int_\Omega (\mu_1^{n+1} v + \delta_t D_1 \nabla \mu_1^{n+1} \cdot \nabla v)\,\mathrm{d}x + \int_\Gamma \delta_t \gamma \mu_1^{n+1} v\,\mathrm{d}x - \sum_{k=1}^{N} \int_{\partial\omega_k} \delta_t \lambda_k^{n+1} v\,\mathrm{d}x \\ - \int_\Omega \mu_1^n v\,\mathrm{d}x - \int_\Omega \delta_t F_1(\mu_1^n, \dots, \mu_{i_0}^n) v\,\mathrm{d}x = 0.\end{aligned} \tag{9}$$

Note that since diffusion is implicit, the source term in the boundary condition is also implicit (λ_k^{n+1}). We evaluate it with a forward Euler scheme, requiring the equation on the monomers to be solved last. In this case we can directly solve

$$\lambda_k^{n+1} - \lambda_k^n = -\delta_t \tau \lambda_k^{n+1} \int_{\Sigma_k^\varepsilon} \mu_{i_0}^{n+1}\,\mathrm{d}x.$$

2. Preliminary theoretical results

The theoretical background allowing for the study of this model will not be formally proved in this work. Further work will provide existence, uniqueness and positivity of solutions.

2.1. **Analytic solution for the healthy state**

Before the spontaneous appearance of the first oligomers (proto-oligomers of size two) in the brain, the system is assumed to rest at a disease-free equilibrium state where only ordinary monomers are present. This configuration is used in the numerical simulations as an initial condition for the distribution of monomers. We hereby present a detailed study of this specific case.

We consider a system composed of one neuron only and assume enough distance between susceptible neuron cells, so that the disease-free resting state of the system for multiple neurons can be computed by the superposition of the multiple solutions for each individual neuron. Moreover, for simplicity in the computation of solutions using polar coordinates we assume the domain Ω to be circular with radius r_Γ. Let Σ be the annular domain between the exterior boundary Γ of radius r_Γ and a circle ω of radius r_N (representing the neuron cell) both centered at the point $(0, 0)$. Let $m(x, t)$ denote the monomer concentration at time t at the point $x \in \Omega$.

In absence of proto-oligomers and oligomers and from the system of equations in Eq. (1), the monomer dynamics follow Eq. (10) given by

$$\frac{\partial m(x,t)}{\partial t} = D_1 \Delta m(x,t) - \delta m(x,t). \tag{10}$$

The corresponding boundary conditions are

$$D_1 \nabla m \cdot \vec{n}|_\Gamma = -\gamma m,$$

at the outer boundary and

$$D_1 \nabla m \cdot \vec{n}|_{\partial\omega} = \lambda_0.$$

In polar coordinates, Eq. (10) becomes

$$\frac{\partial m(x,t)}{\partial t} = D_1 \left(\frac{\partial^2 m(r,\theta,t)}{\partial r^2} + \frac{1}{r}\frac{\partial m(r,\theta,t)}{\partial r} + \frac{1}{r^2}\frac{\partial^2 m(r,\theta,t)}{\partial \theta^2} \right) - \delta m(r,\theta,t), \tag{11}$$

with Neumann boundary conditions

$$\begin{aligned} D_1 \frac{\partial m(r_\Gamma,\theta,t)}{\partial r} &= -\gamma m(r_\Gamma,\theta,t), \\ D_1 \frac{\partial m(r_N,\theta,t)}{\partial r} &= -\lambda_0. \end{aligned}$$

with $0 < r_N \leq r \leq r_\Gamma$. Notice that the normal vector is pointing out of Ω so the sign is reversed in r_N $(-\lambda_0)$.

The problem is symmetrical by rotation around $(0,0)$ thanks to the choice of concentrical circles for the different boundaries, so as long as the initial condition does not depend on θ (in polar coordinates), the solution will keep this symmetry at all times. Using this assumption on the initial condition, we drop the dependency on θ in the following and write $m(x,t) = m(r,t)$. The partial differential equation becomes

$$\frac{\partial m(r,t)}{\partial t} = D_1 \left(\frac{\partial^2 m(r,t)}{\partial r^2} + \frac{1}{r}\frac{\partial m(r,t)}{\partial r} \right) - \delta m(r,t),$$

with the new boundary conditions

$$\begin{aligned} D_1 \frac{\partial m(r_\Gamma,t)}{\partial r} &= -\gamma m(r_\Gamma,t), \\ D_1 \frac{\partial m(r_N,t)}{\partial r} &= -\lambda_0. \end{aligned}$$

To find the equilibrium solution $m_0(r)$ we set

$$D_1 \left(m_0''(r) + \frac{1}{r} m_0'(r) \right) - \delta m_0(r) = 0,$$

with

$$\begin{aligned} D_1 m_0'(r_\Gamma) + \gamma m_0(r_\Gamma) &= 0, \\ D_1 m_0'(r_N) + \lambda_0 &= 0. \end{aligned}$$

This equation can then be written in the form of an Emden-Fowler equation or a Sturm-Liouville equation [1]

$$\frac{\mathrm{d}}{dr}\left(r \frac{dm_0}{\mathrm{d}r}(r) \right) - r\frac{\delta m_0(r)}{D_1} = 0.$$

Its solution exists and has the form [10, 11]

$$m_0(r) = c_1 J_0\left(\frac{\mathrm{i}\sqrt{\delta} r}{\sqrt{D_1}} \right) + c_2 Y_0\left(-\frac{\mathrm{i}\sqrt{\delta} r}{\sqrt{D_1}} \right) \tag{12}$$

with c_1 and c_2 constants depending on the boundary conditions and J_0 and Y_0 Bessel functions of the first and second kind respectively. In practice, this steady-state problem will be solved numerically in order to determine the initial condition for the evolution problem. This theoretical study provides the possibility of comparison with the numerical solution, as well as qualitative analysis of the various parameters on the disease-free solution.

3. Numerical results

3.1. Parameter choice and model scaling

3.1.1. *Non-dimensional equations*

To ease the numerical simulation, we nondimensionalize the model. First we specify the unit system we use. In the following we consider SI units. In particular, we express lengths in meters and time in seconds. For concentrations we use the molar concentration unit M ($1M = 1\ mol.L^{-1}$). We can now define the scales.

- Spatial scale: we define L the characteristic length of the domain. Typically L is about 100 μm.
- Time scale: the characteristic time is T, it is about 100 s.
- Concentration scales: the characteristic concentration is C_0, around $10^{-9}M$.

Using these scales we can nondimensionalize the model. In the rest of this section, a superscript $*$ will indicate nondimensional variables. We define

$$t^* = \frac{t}{T}, x^* = \frac{x}{L}, y^* = \frac{y}{L}, \xi^* = \frac{\xi}{C_0}, \xi = \mu_1, \dots, \mu_{i_0}. \tag{13}$$

The non-dimensional operators are given by

$$\begin{aligned} \frac{\partial}{\partial t} =& \frac{1}{T}\frac{\partial}{\partial t^*}, \\ \nabla =& \frac{1}{L}\nabla^*, \\ \Delta =& \frac{1}{L^2}\Delta^*. \end{aligned} \tag{14}$$

Now using the equations of the model, we obtain the nondimensional model. The equations are the same as (1), replacing the operators by the non-dimensional operators and modifying the coefficients as follows

$$D^* = D\frac{T}{L^2},\ r_i^* = r_i C_0 T,\ b^* = bT,\ \beta^* = \beta T,\ \delta^* = \delta T,\ \gamma^* = \gamma\frac{T}{L},\ \lambda_k^* = \lambda_k \frac{T}{LC_0},\ \tau^* = \tau C_0 T.$$

3.1.2. *Parameter choices*

To be consistent with biology we need to choose the coefficients appropriately. We know from anatomy that neurons have a size of a few μm and are separated by around 10 μm in the brain. Accordingly, the characteristic spatial scale will be $L = 100\ \mu m$.

For specific data on Aβ, we refer to [20]. The diffusion coefficients will be chosen using the Stokes-Einstein relation

$$D = \frac{k_b T}{6\pi\mu r_h},$$

where k_b is the Boltzmann constant ($k_b = 1.38.10^{-23}\ m^2 kg s^{-2} K^{-1}$), T the temperature, μ the dynamical viscosity of the fluid, and r_h the hydrodynamic radius of the particle considered. In the case of Aβ particles in the cerebrospinal fluid we have (in SI units) $T = 310\ K(37°C)$, $\mu = 10^{-3}\ kgm^{-1}s^{-1}$ [4]. The hydrodynamic radius of monomers is $r_h = 1\ nm$ [21]. For oligomeric species, the hydrodynamic radius grows with the size and we suggest it scales as $i^{1/3}$ where i is the size of the oligomers (to represent 3D rearrangement of the particle as it grows in size). This ultimately gives $D_1 = 2.27.10^{-10}\ m^2 s^{-1}$, and $D_i = \frac{D_1}{i^{1/3}}$. This value is of the same order as measured by [20]. However when we use this value for the diffusion coefficient in the simulations, the distribution of Aβ monomers in the spatial scale $L \approx 100\ \mu m$ is almost homogeneous. To obtain a significant variation of the monomer distribution on this scale, the diffusion coefficient has to be reduced to $D \approx 10^{-14}\ m^2.s^{-1}$. This in turn corresponds to a displacement of 1 μm in approximately 10 s. To justify the use of a diffusion coefficient 4 orders

of magnitude than the one suggested by the Stokes-Einstein formula, we first suggest that the cerebrospinal fluid is very crowded by other proteins and assemblies, which impairs the diffusion of molecules. Furthermore, the spatial spreading of the neurons could be increased in the model, because *in vivo* not all the neurons produce Aβ. Without more detailed data, we choose to use $D \approx 10^{-14}\ m^2.s^{-1}$.

For the production and degradation of monomers, we have some suggestions from literature [20, 21]. The disease-free equilibrium concentration of Aβ monomers in the cerebrospinal fluid is of about $C_b = 10\ ng.mL^{-1}$ [18]. The molecular weight of Aβ is 4514 $g.mol^{-1}$, so this concentration amounts to about $C_b = 2.10^{-9}\ M$. The half-life of Aβ monomers is a few hours, which corresponds to a degradation rate δ of about $10^{-4}\ s^{-1}$. The total production rate of a disease-free neuron (integrated over its surface) is $\lambda_0 \pi R^2_{\text{neuron}}$. If we consider that the measured concentration in the cerebrospinal fluid is equivalent to that of a single neuron in a domain of volume $V_{\text{neuron}} = 20\ \mu m^3$, the equilibrium between production and degradation gives us the relation $\lambda_0 \pi R^2_{\text{neuron}}/V = C_b\delta = 2.10^{-13}\ M.s^{-1}$, from which we evaluate λ_0.

The polymerization-depolymerization reaction is estimated to occur at rates $r_0 = 100\ M^{-1}s^{-1}$ and $b = 10^{-3}\ s^{-1}$. The fragmentation rate is more difficult to evaluate, it will be adjusted using the simulations. The same goes for γ and τ. The parameter choices are summarized in Table 1.

TABLE 1. Parameter values used for the simulations (unless specified otherwise). See the main text for a detailed justification of the parameter choice.

Parameter	Value	Unit	Description
T	50000	s	Time scale
L	100	μm	Length scale
C_0	10^{-9}	M	Concentration scale
i_0	20	-	Size of oligomers
D_i	$D_1/i^{1/3}$	$m^2.s^{-1}$	Diffusion coefficient of size i
D_1	$2.2.10^{-14}$	$m^2.s^{-1}$	Diffusion coefficient of monomers
δ	5.10^{-4}	s^{-1}	Degradation coefficient of monomers
γ	1	$m.s^{-1}$	Surface absorption rate
r_i	r_0	$M^{-1}s^{-1}$	Polymerization rate of size i
r_0	10^7	$M^{-1}s^{-1}$	Basal poplymerization rate
b	10^{-3}	s^{-1}	Depolymerization rate
β	10^{-4}	s^{-1}	Fragmentation rate
$\lambda_0 \times \pi R^2_{\text{neuron}}/V_{\text{neuron}}$	2.10^{-13}	$M.s^{-1}$	Monomer production rate of a neuron
τ	10^{10}	$M^{-1}.s^{-1}$	Infectivity rate
R_{neuron}	2	μm	Radius of a neuron
V_{neuron}	20	μm^3	Apparent volume of isolation for a neuron
ε	2	μm	Radius of activity for oligomers

3.2. **Simulation results**

The numerical resolution of the model is conducted using Freefem++ [14], and visualized in Paraview [2]. The default parameter values are presented in Table 1, and the initial configuration for all the simulations is presented in Figure 3.

Figure 4 shows the results of the simulation with the default parameters (see Table 1). We observe the successive attacks of oligomers first on the left neuron, then the right neuron. Their monomer production is progressively brought to 0 and after about 20000 s, both of the neurons are completely inactive. The balance between diffusion and replication of the proto-oligomers plays a critical role in the observed dynamics. The spatial distribution of the oligomers is strongly impacted, and their neurotoxic action is also affected. It appears that there is an optimal value for the rate of fragmentation β that induces the fastest neuron inactivation. With

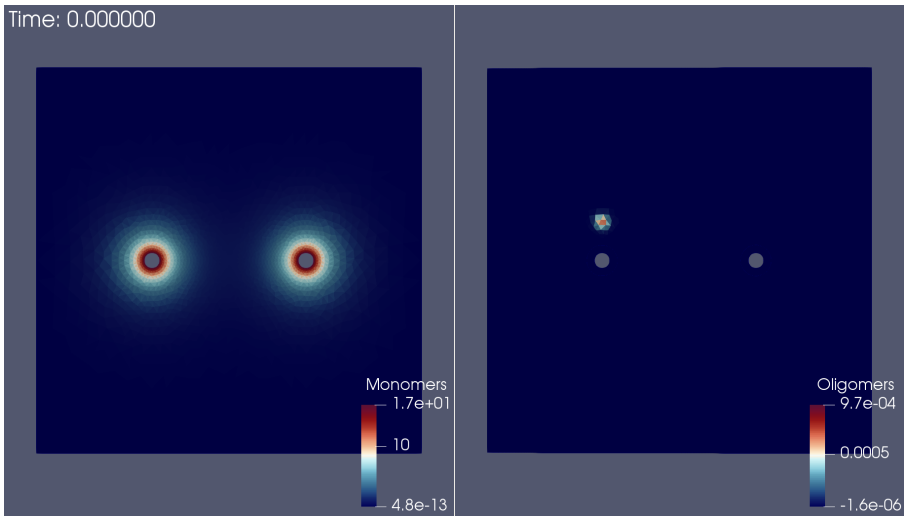

FIGURE 3. Initial configuration used for the simulation. Left panel: Aβ monomer distribution. Right panel: Aβ oligomers (of size i_0) distribution.

extremely high fragmentation rates ($\beta > 5.10^{-3}\ s^{-1}$), the oligomers reach both neurons, but their concentration does not reach sufficiently high levels to completely inactivate them in less than 50000 s, as shown in Figure 5. With extremely low fragmentation rates ($\beta < 10^{-5}\ s^{-1}$) the proto-oligomer distribution is shifted towards larger, so they diffuse more slowly. In this case, the first neuron is inactivated efficiently enough, but the second is still producing at half the maximum rate after 50000 s, see Figure 6.

4. Conclusion and perspectives

This preliminary work has allowed us to build a promising model to study the spatial propagation Aβ oligomers during the early stages of AD. The model is very restrictive, because it focuses on the scale of a few neurons and a few hours. These limitations lead to a simpler model than suggested by previous work [3]. Nevertheless, despite its simplicity, it already exhibits some complex behavior and non-trivial parameter dependence. In particular, the fragmentation rate of proto-oligomers appears to be critical in determining the dynamics of oligomers and their efficiency at inactivating neurons. Further study of this model is planned; first by establishing a theoretical framework (existence, uniqueness, positivity of the solutions), and by extending the simulations to more complex cases, *e.g.* adding more neurons to the domain. Also, investigating thoroughly the influence of the parameters (including, but not limited to, the fragmentation rate), as well as that of the initial conditions. Moreover, including a more detailed description of the neurotoxicity of the oligomers and extending this model to a multi-scale model of the propagation of AD, taking into account fibrils, plaques and macroscopical processes.

5. Acknowledgements

We express our thanks to the organizing team of CEMRACS 2018 and SMAI for the opportunity to participate in this event and to start this project. We also thank Human Rezaei (INRA, Jouy-en-Josas) for fruitful discussions and his great help in the choice of the parameters.

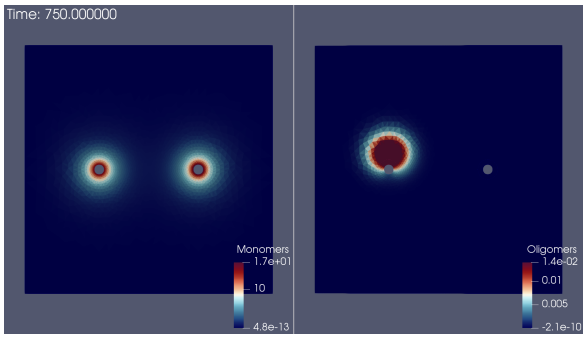

(A) $t = 750\ s$

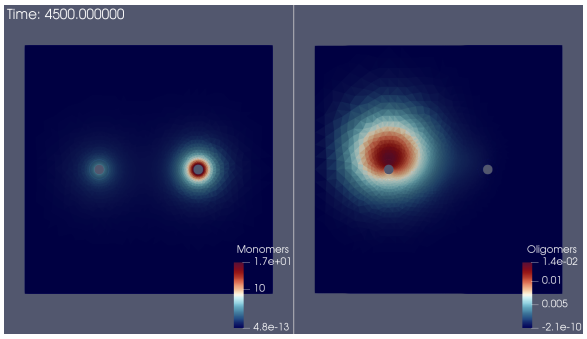

(B) $t = 4500\ s$

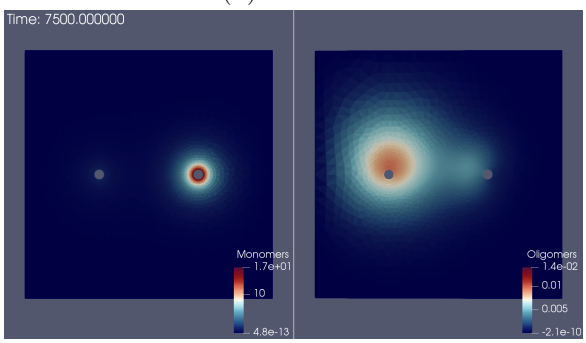

(C) $t = 7500\ s$

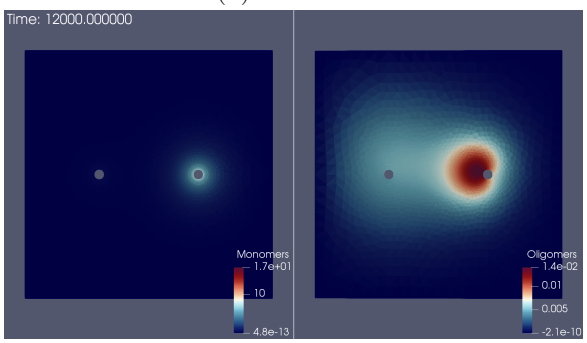

(D) $t = 12000\ s$

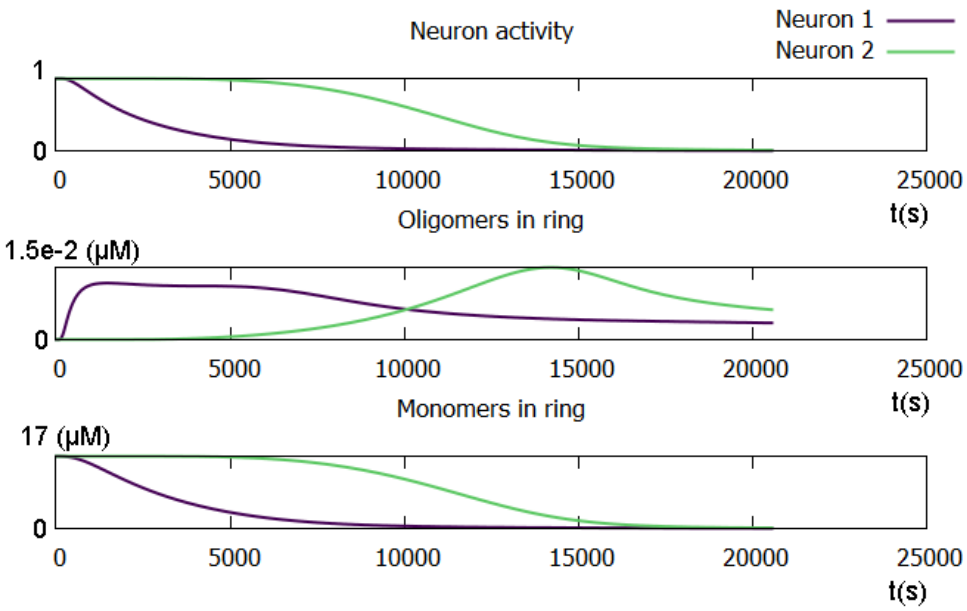

(E) Evolution of monomer production normalized by the maximum λ_0 (top), oligomer concentration in activity ring (middle) and monomer concentration in ring (bottom) for each neuron and over time.

FIGURE 4. Simulation results for the default parameters (see Table 1). For panels (a),(b),(c) and (d), the monomer distribution is on the left, and the oligomer distribution is on the right.

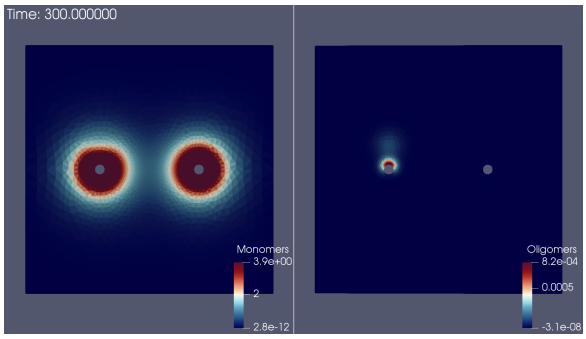

(A) $t = 300\ s$

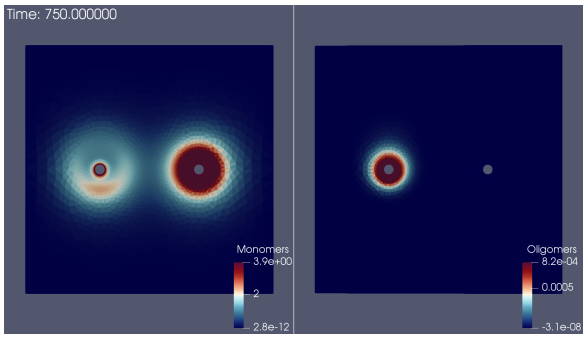

(B) $t = 750\ s$

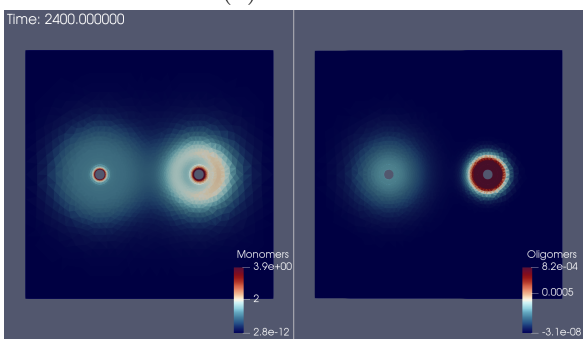

(C) $t = 2400\ s$

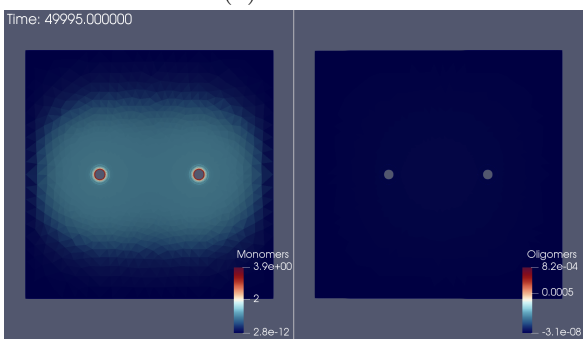

(D) $t = 49995\ s$

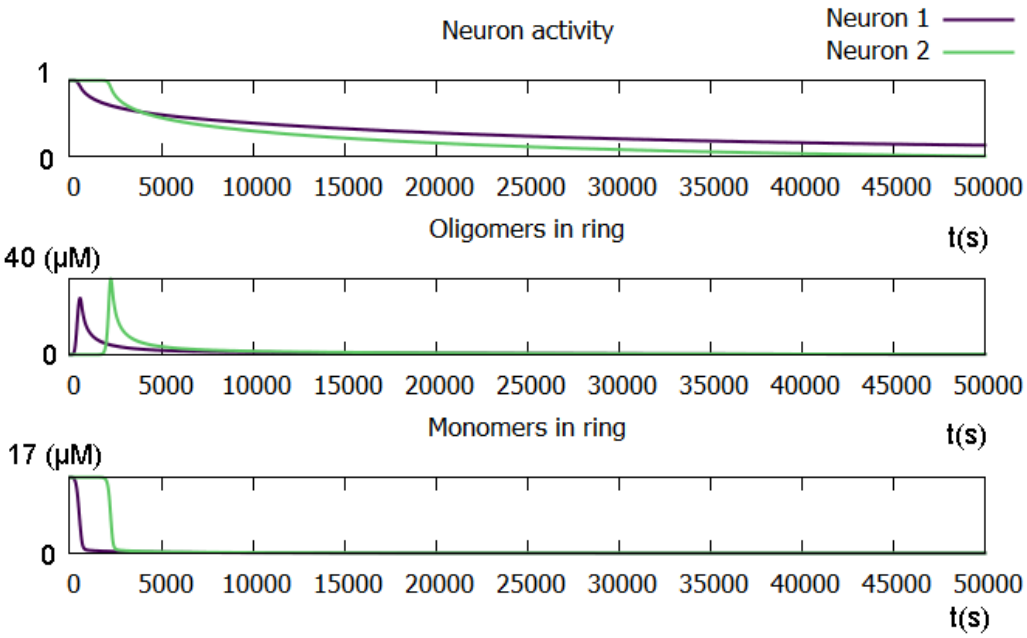

(E) Evolution of monomer production normalized by the maximum λ_0 (top), oligomer concentration in activity ring (middle) and monomer concentration in ring (bottom) for each neuron and over time.

FIGURE 5. Simulation results for $\beta = 5.10^{-3}\ s^{-1}$ (see Table 1 for the other paramters). For panels (a),(b),(c) and (d), the monomer distribution is on the left, and the oligomer distribution is on the right.

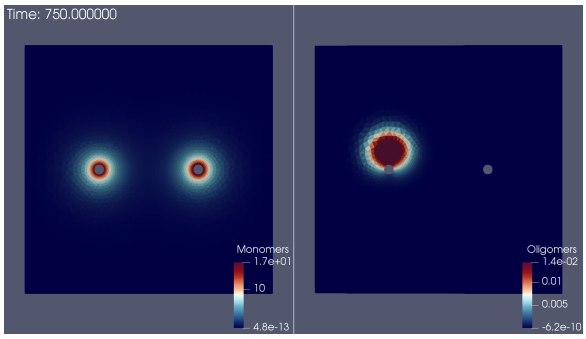

(A) $t = 750\ s$

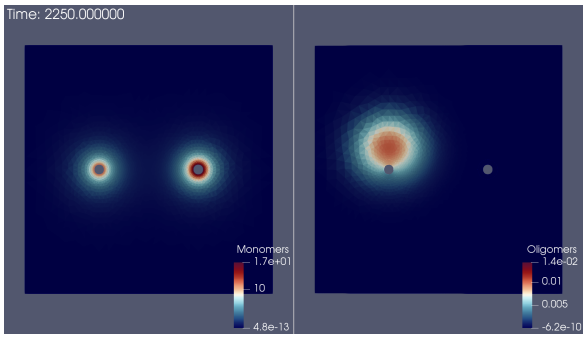

(B) $t = 2250\ s$

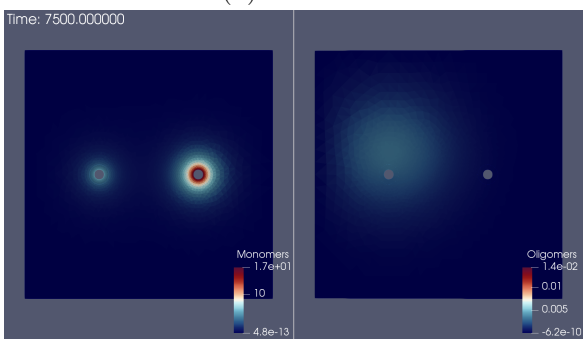

(C) $t = 7500\ s$

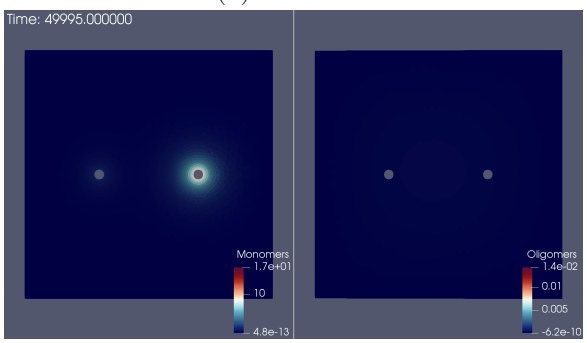

(D) $t = 49995\ s$

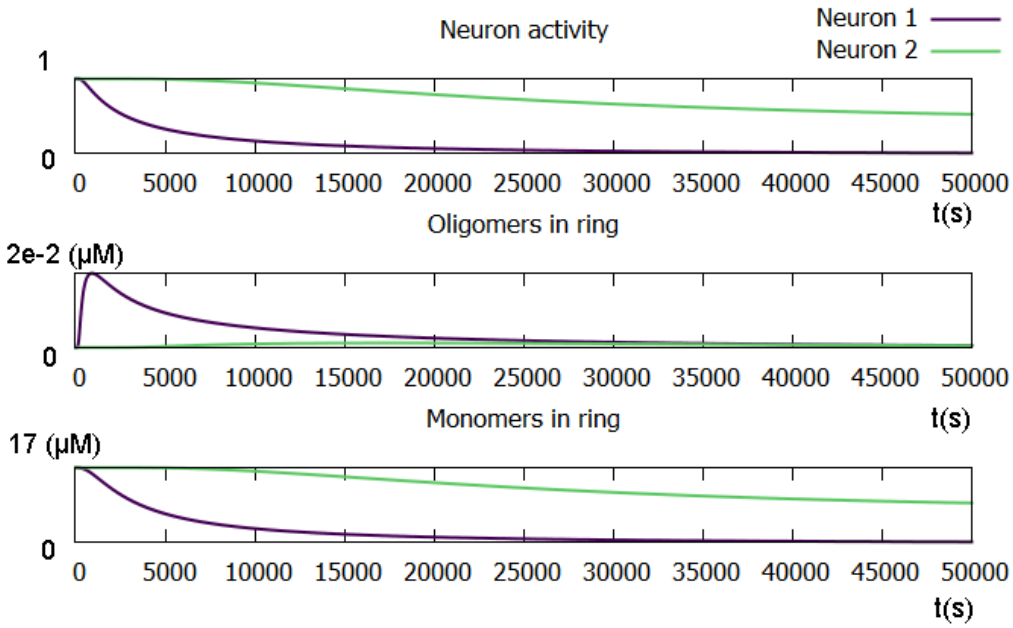

(E) Evolution of monomer production normalized by the maximum λ_0 (top), oligomer concentration in activity ring (middle) and monomer concentration in ring (bottom) for each neuron and over time.

FIGURE 6. Simulation results for $\beta = 1.10^{-5}\ s^{-1}$ (see Table 1 for the other paramters). For panels (a),(b),(c) and (d), the monomer distribution is on the left, and the oligomer distribution is on the right.

References

[1] G. B. Arfken and H. J. Weber. Mathematical methods for physicists, 1999.

[2] U. Ayachit. The paraview guide: a parallel visualization application. 2015.

[3] M. Bertsch, B. Franchi, N. Marcello, M.C. Tesi, and A. Tosin. Alzheimer's disease: a mathematical model for onset and progression. *Mathematical medicine and biology: a journal of the IMA*, 34(2):193–214, 2016.

[4] I.G. Bloomfield, I.H. Johnston, and L.E. Bilston. Effects of proteins, blood cells and glucose on the viscosity of cerebrospinal fluid. *Pediatric neurosurgery*, 28(5):246–251, 1998.

[5] F. Carbonell, Y. Iturria-Medina, and A.C. Evans. Mathematical modeling of protein misfolding mechanisms in neurological diseases: a historical overview. *Frontiers in Neurology*, 9:37, 2018.

[6] I.S. Ciuperca, M. Dumont, A. Lakmeche, P. Mazzocco, L. Pujo-Menjouet, H. Rezaei, and L.M. Tine. Alzheimer's disease and prion: analysis of an in vitro mathematical model. 2016.

[7] S.I.A. Cohen, S. Linse, L.M. Luheshi, E. Hellstrand, D.A. White, L. Rajah, D.E. Otzen, M. Vendruscolo, C.M. Dobson, and T.P.J. Knowles. Proliferation of amyloid-β42 aggregates occurs through a secondary nucleation mechanism. *Proceedings of the National Academy of Sciences*, 110(24):9758–9763, 2013.

[8] M. Doumic, T. Goudon, and T. Lepoutre. Scaling limit of a discrete prion dynamics model. *Commun. Math. Sci.*, 7(4):839–865, 2009.

[9] S. Eleuteri, S. Di Giovanni, E. Rockenstein, M. Mante, A. Adame, M. Trejo, W. Wrasidlo, F. Wu, P.C. Fraering, E. Masliah, et al. Blocking Aβ seeding-mediated aggregation and toxicity in an animal model of Alzheimer's Disease: A novel therapeutic strategy for neurodegeneration. *Neurobiology of disease*, 74:144, 2015.

[10] W. N. Everitt. A catalogue of Sturm-Liouville differential equations. In *Sturm-Liouville Theory*, pages 271–331. Springer, 2005.

[11] W.N. Everitt and C. Markett. On a generalization of bessel functions satisfying higher-order differential equations. *Journal of Computational and Applied Mathematics*, 54(3):325–349, 1994.

[12] M.L. Greer, L. Pujo-Menjouet, and G.F. Webb. A mathematical analysis of the dynamics of prion proliferation. *Journal of theoretical biology*, 242(3):598–606, 2006.

[13] C. Haass and D.J. Selkoe. Soluble protein oligomers in neurodegeneration: lessons from the Alzheimer's amyloid β-peptide. *Nature reviews Molecular cell biology*, 8(2):101, 2007.

[14] F. Hecht. New development in FreeFem++. *J. Numer. Math.*, 20(3-4):251–265, 2012.

[15] M. Helal, E. Hingant, L. Pujo-Menjouet, and G.F. Webb. Alzheimers disease: analysis of a mathematical model incorporating the role of prions. *Journal of mathematical biology*, 69(5):1207–1235, 2014.

[16] M. Helal, A. Igel-Egalon, A. Lakmeche, P. Mazzocco, A. Perrillat-Mercerot, L. Pujo-Menjouet, H. Rezaei, and L. M. Tine. Stability analysis of a steady state of a model describing Alzheimers disease and interactions with prion proteins. *Journal of mathematical biology*, pages 1–25, 2018.

[17] J. Masel, V. A.A. Jansen, and M. A. Nowak. Quantifying the kinetic parameters of prion replication. *Biophysical chemistry*, 77(2-3):139–152, 1999.

[18] P.D. Mehta, T. Pirttilä, S.P. Mehta, E.A. Sersen, P.S. Aisen, and H.M. Wisniewski. Plasma and cerebrospinal fluid levels of amyloid β proteins 1-40 and 1-42 in Alzheimer disease. *Archives of neurology*, 57(1):100–105, 2000.

[19] R. Morales, C. Duran-Aniotz, J. Castilla, L.D. Estrada, and C. Soto. De novo induction of amyloid-β deposition in vivo. *Molecular psychiatry*, 17(12):1347, 2012.

[20] R.M. Murphy and M.M. Pallitto. Probing the kinetics of β-amyloid self-association. *Journal of structural biology*, 130(2-3):109–122, 2000.

[21] S. Nag, B. Sarkar, A. Bandyopadhyay, B. Sahoo, V.K.A. Sreenivasan, M. Kombrabail, C. Muralidharan, and S. Maiti. The nature of the amyloid-β monomer and the monomer-oligomer equilibrium. *Journal of Biological Chemistry*, pages jbc–M110, 2011.

[22] T.T. Olsson, O. Klementieva, and G.K. Gouras. Prion-like seeding and nucleation of intracellular amyloid-β. *Neurobiology of disease*, 113:1–10, 2018.

[23] U. Sengupta, A.N Nilson, and R. Kayed. The role of amyloid-β oligomers in toxicity, propagation, and immunotherapy. *EBioMedicine*, 6:42–49, 2016.

[24] C. Soto. Unfolding the role of protein misfolding in neurodegenerative diseases. *Nature Reviews Neuroscience*, 4(1):49, 2003.

[25] R.F. Sowade and T.R. Jahn. Seed-induced acceleration of amyloid-β mediated neurotoxicity in vivo. *Nature communications*, 8(1):512, 2017.

[26] A. Vasseur, F. Poupaud, J.-F. Collet, and T. Goudon. The Beker–Döring System and Its Lifshitz–Slyozov Limit. *SIAM Journal on Applied Mathematics*, 62(5):1488–1500, 2002.

[27] T. Xiao, W. Zhang, B. Jiao, C.-Z. Pan, X. Liu, and L. Shen. The role of exosomes in the pathogenesis of Alzheimerdisease. *Translational neurodegeneration*, 6(1):3, 2017.

[28] R. Yvinec, J. Deschamps, and E. Hingant. From Becker-Döring to Lifshitz-Slyozov: deriving the non-local boundary condition of a non-linear transport equation. In *ITM Web of Conferences*, volume 5, page 00017. EDP Sciences, 2015.